Review Vol. 14, No. 10 / 1 Oct 2023 / Biomedical Optics Express 5451
Biomedical Optics EXPRESS

Harnessing the power of optical microscopy for visualization and analysis of histopathological images

NAN WANG,[1,2] CHANG ZHANG,[1] XINYU WEI,[1] TIANYU YAN,[1,2] WANGTING ZHOU,[1,2,5] JIAOJIAO ZHANG,[1,2] HUAN KANG,[1,2] ZHEN YUAN,[3,6] AND XUELI CHEN[1,2,4,*]

[1]*Center for Biomedical-photonics and Molecular Imaging, Xi'an Key Laboratory of Intelligent Sensing and Regulation of Trans-Scale Life Information, School of Life Science and Technology, Xidian University, Xi'an, Shaanxi 710126, China*
[2]*Engineering Research Center of Molecular and Neuro Imaging, Ministry of Education, Xi'an, Shaanxi 710126, China*
[3]*Faculty of Health Sciences, University of Macau, Macau, 999078, China*
[4]*Inovation Center for Advanced Medical Imaging and Intelligent Medicine, Guangzhou Institute of Technology, Xidian University, Guangzhou, Guangdong 510555, China*
[5]*wtzhou@xidian.edu.cn*
[6]*zhenyuan@um.edu.mo*
[*]*xlchen@xidian.edu.cn*

Abstract: Histopathology is the foundation and gold standard for identifying diseases, and precise quantification of histopathological images can provide the pathologist with objective clues to make a more convincing diagnosis. Optical microscopy (OM), an important branch of optical imaging technology that provides high-resolution images of tissue cytology and structural morphology, has been used in the diagnosis of histopathology and evolved into a new disciplinary direction of optical microscopic histopathology (OMH). There are a number of *ex-vivo* studies providing applicability of different OMH approaches, and a transfer of these techniques toward *in vivo* diagnosis is currently in progress. Furthermore, combined with advanced artificial intelligence algorithms, OMH allows for improved diagnostic reliability and convenience due to the complementarity of retrieval information. In this review, we cover recent advances in OMH, including the exploration of new techniques in OMH as well as their applications, and look ahead to new challenges in OMH. These typical application examples well demonstrate the application potential and clinical value of OMH techniques in histopathological diagnosis.

1. Introduction

Histopathological analysis has emerged from the growing need for multi-informative analysis of diseases, and has been greatly improved and developed over past decades. It plays a critical role in cancer diagnosis and treatment, which is performed intraoperatively or diagnostically to provide visualization of high-resolution microscopic structures and morphology of tissues [1]. Histopathological images show tissue types and identify the histopathology difference between cancerous tissue and healthy tissue, or necrotic tissue and surviving tissue. Besides, histopathology not only helps to guide surgeons in excising cancerous tissue while preserving organ function, but can also assists in determining adjuvant treatments, as well as diagnosing, grading, and staging malignant tumors. The current "gold standard" for histopathological analysis is formalin-fixed paraffin-embedded (FFPE) followed by hematoxylin and eosin (H&E) staining and microscopic imaging [2]. Recently, with the rapid progress of cryogenic technology, frozen section analysis has emerged as a potential technique. There are significant differences from conventional methods, but the basis of FFPE and frozen methods is equivalent. First, the excised

#501893 https://doi.org/10.1364/BOE.501893
Journal © 2023 Received 27 Jul 2023; revised 29 Aug 2023; accepted 1 Sep 2023; published 26 Sep 2023

Biomedical Optics EXPRESS

pathological tissues are deposited into a substrate to form a solid tissue block [3], and thin tissue slices are then shaved from the block using a microtome. Finally, the thin slices are stained by the pathologist and histologically examined under a microscope. This enables visualization that is compatible with traditional transmission light microscopy. However, despite the high impact of this conventional histopathological imaging, it has some major drawbacks. First, the processing of all procedures is time-consuming and cumbersome, which can delay diagnosis by days or even weeks in some instances [4]. Second, the thin slices require high precision, sometimes necessitating multiple attempts to recover an adequate slice. Third, histopathological images are color inconsistency that may significantly affect image analysis and diagnosis [4]. In addition, due to the serious lack of experienced pathologists in most of the world, they need to check a large number of pathological slides every day. Thus, there is an urgent need for a way to help pathologists reduce time-consuming and labor-intensive diagnosis tasks [5]. Advances in OM and artificial intelligence have contributed to the renaissance of histopathological image visualization and analysis. Use of OM as an analytical tool is of a significant interest because it allows for noninvasive and nonionizing sample investigation with high spatial resolution under ambient conditions [6].

Recently, a series of OM techniques have emerged and demonstrated remarkable results toward visualization and analysis of tissues [7–14]. Similar to the contrast provided by the H&E staining, it can be obtained from unstained tissues in a label-free manner, including FFPE tissue blocks, FFPE tissue slices, and frozen slices. At the same time, these techniques would not modify samples during imaging, preserving tissues for further immunohistochemical analysis. Visualizing tissue morphology directly on preserved samples can reduce the requirements for slicing and staining, saving time and resources. Thus far, there are several practical hurdles that have prevented direct histology-like imaging of unstained FFPE and frozen preparations. In addition, capturing high-fidelity tissue features without exogenous contrast agents is also a significant hurdle [2]. The most popular techniques such as fluorescence microscopy [7], light sheet microscopy [8], lens-free computational microscopy [9], and polarization microscopy [10], can visualize histopathological images but requires exogenous dyes in most cases. Conversely, recent advances in OM techniques, including photoacoustic microscopy [11], coherent Raman scattering microscopy [12], optical coherence tomography [13], and two-photon microscopy [14] have highlighted other possibilities for histopathological imaging in a label-free manner. They have been applied to histological imaging in a variety of preserved samples. Due to the significant advantages of OM techniques in histological imaging and its successful application in histopathology, it has evolved into a new disciplinary direction of OMH.

In this review, we summarize the advances in OMH techniques, involving the exploration of new technical implementations in OMH, and their applications in cells and tissues selected from recent, respective literatures. These typical application examples well demonstrate the application potential and powerful value of new OMH techniques in clinical histopathological diagnosis. In the end, we look ahead to some new challenges in OMH and enhance its powerful alternative to the field.

2. Advances in optical microscopic histopathology

Histopathological imaging and analysis of thin tissue slices is an essential tool for disease diagnosis, tumor excision, and other malignancies. Current histopathological imaging techniques require extensive sample processing before staining, to highlight the tissue morphology. However, sample preparation and staining are resource intensive and introduce the possibility of variability. As an emerging disciplinary direction, OMH may offer a new alternative to address the above issues. In the last decade, more and more OMH techniques have been explored and used for histopathological imaging, for example the laser scanning fluorescence microscopy (LSFM), photoacoustic microscopy (PAM), coherent Raman microscopy (CRM), light sheet

Biomedical Optics EXPRESS

microscopy (LSM), ultraviolet microscopy (UVM), lens-free computational microscopy (LFCM), polarization microscopy (PM), and Fourier ptychography microscopy (FPM), *etc*. These technologies can be divided into different categories according to different classification criteria. For example, depending on how the images are acquired, OMH can be classified into direct optical microscopic histopathology (dOMH) and computational optical microscopic histopathology (cOMH). According to the formation of the images, OMH can be divided into point-scanning, line-scanning, and wide-field microscopy. Depending on the source that generates the signal, OMH can be refined into different types of fluorescent-, Raman-, phased-, polarized-type, *etc*. In this review, we summarized the OMH techniques using a classification according to how the images were acquired. The OMH technique outlined in this paper is shown in Fig. 1 below.

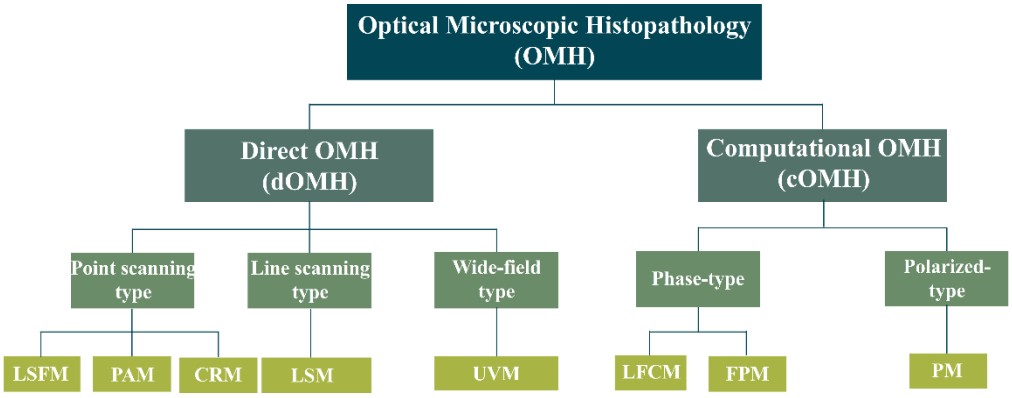

Fig. 1. The outline of optical microscopic histopathology technology.

2.1. Direct optical microscopic histopathology

dOMH is a WYSIWYG (what you see is what you get) technique in which the entire sample field of view is scanned and a whole image of the sample is directly available at the detection end. Details of the physics of these techniques can be found in various textbooks [15–27]. This section covers some fundamental aspects of these techniques including LSFM, PAM, CRM, LSM, UVM, following the instrumentation as well as their applications for histopathological slides.

2.1.1. Laser scanning fluorescence microscopy

LSFM presents an appealing tool to probe biological processes with better signal-to-noise ratio, spatial resolution, and optical sectioning than wide-field fluorescence microscopy. There are several representative implementations, including the laser scanning confocal fluorescence microscopy (LSCFM), auto-fluorescence microscopy (AFM), and multiphoton fluorescence microscopy (MPFM, including two-photon fluorescence microscopy and three-photon fluorescence microscopy). Current instrumentation of LSFM operates in a conjugate configuration, which effectively suppresses inter-pixel interference and improves image quality. Moving the sample stage or deflecting the illumination beam, LSFM enables adjustable focused light to achieve selective illumination and detection of the sample. LSCFM employs a pinhole, conjugating with a confocal spot, to block out-of-focus signal by placing at the front of the signal detector [15]. AFM has rich endogenous fluorophores, including reduced nicotinamide adenine dinucleotide, structural proteins (e.g., collagen and elastin), aromatic amino acids (e.g., tryptophan, tyrosine), and heterocyclic compounds (e.g., flavins, flavoprotein, and lipochrome), *etc*. It can be used for cell monitoring and disease diagnosis by means of the changes of cell morphology, cell

Biomedical Optics EXPRESS

metabolism, and pathological state [16]. MPFM has a high penetration depth and low phototoxicity, making it the method of choice for long-term continuous visualization of deep *in vivo* imaging [14,17,18]. It excites fluorescent signals only in the region near the focal point of the excitation light and has a natural chromatography ability to better image biological tissues.

In 2020, Chacko *et al.* used the reduced nicotinamide adenine dinucleotide endogenous fluorescence to extract microenvironment information in fixed tissues, demonstrating that the use of auto-fluorescence to distinguish metabolism and PH changes has great pathological value [19]. LSCFM enables to identify morphologic and cellular features of benign and cancerous lesions [20–22]. Italian pathologists performed LSCFM on fresh surgical sections of 30 patients, including 4 types of histopathological blocks such as masses, thyroid, and others. The results were highly consistent with H&E staining, demonstrating its strong potential for rapid pathological examination of intraoperative tissue sections [23]. Combined with endoscopy or miniaturization techniques, LSFM can also be used to perform *in vivo* high-resolution optical biopsies on patients. Li *et al.* reported a needle-based confocal laser endomicroscopy (CLE) for gastric subepithelial tumors, whose results demonstrated that it can generate 500-1000 magnification virtual histological images of tissue without adequate tissue preparation [24]. Besides, CLE has also been used for neurosurgery diagnoses, such as the precise diagnosis of gliomas and their surrounding microenvironment. Qin *et al.* developed a two-photon endomicroscope that adds adaptive optics to direct wavefront sensing, thereby restoring diffraction-limited resolution in deep brain imaging [25]. Figure 2 shows representative results of different LSFM and H&E staining of tumor tissue slices [19,24,26,27].

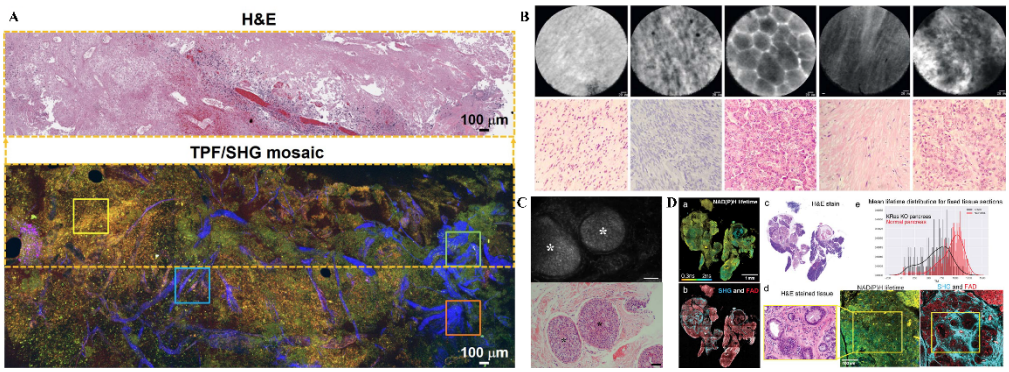

Fig. 2. Representative results of LSFM-based histopathologic imaging. (A) Mosaic image (bottom) of unlabeled fresh high-grade glioma tissue and roughly co-located H&E histology (top) in the dotted line rectangle, where square regions marked with different colors are region of necrosis (yellow), extensive microvascular proliferation (blue), thrombosed vessel (red), and direct collagen deposition (green), respectively. Adapted with permission from [27]. (B) CLE (top panel) and the corresponding histological images (bottom panel). Adapted with permission from [24] ©Georg Thieme Verlag KG. (C) LSCFM result (top panel) and H&E staining imaging result (bottom panel) of *in situ* ductal carcinoma tissue section. Adapted with permission from Springer Nature: [26]. (D) Comparison of AFM, SHG&FAD, and H&E staining results of pancreatic tissue. Reproduced with permission from [19] © IOP Publishing Ltd. (TPF: two-photon fluorescence; SHG: second harmonic generation; FAD: Flavin adenine dinucleotide.)

2.1.2. Photoacoustic microscopy

Over the past decade, photoacoustic imaging has been introduced primarily in biomedical applications. PAM, as an important branch of photoacoustic imaging, has also shown great

Biomedical Optics EXPRESS

potential in clinical diagnosis. The first-generation PAM, developed by Wang *et al.*, can reveal physiological features by providing multi-scale information [28]. Subsequently, there are various PAMs were developed [29], such as 3D handheld photoacoustic imager, and high-resolution non-invasive photoacoustic dermoscopy. According to the focusing medium, PAM can be divided into optical-resolution PAM (OR-PAM) and acoustic-resolution PAM (AR-PAM). In OR-PAM, the focused light with one pulse laser wavelength induces acoustic signal from biological tissue, which is detected by a focused ultrasound transducer. The optical focusing objective lens and the focused ultrasonic detector are generally focused on the coaxial, and the maximum detection sensitivity can be achieved by confocal excitation and detection. The lateral resolution of a few microns is determined by the diameter of the focused light, and the axial resolution of tens of microns can be achieved by using a high-frequency, wide bandwidth ultrasonic transducer.

PAM has become a promising optical biopsy method for clinical diagnosis, including brain neuroimaging, brain tumors, skin cancers, obesity-induced cerebrovascular alterations, port-wine-stained skin disease, and pathological sections analysis, *etc*. [30,31]. Recent advances in PAM technique has highlighted other possibilities for histopathological diagnosis. Wang *et al.* developed an ultraviolet PAM that can perform real-time three-dimensional contour scanning of tissues in refection mode for rapid diagnosis of bone tissue lesions. Experimental results validated with H&E-stained imaging revealed that the technique can be used for intraoperative evaluation of thick uncalcified and decalcified bone specimens [32]. Benjamin *et al.* developed a dual-contrast photoacoustic remote sensing (PARS) microscopy for histopathological assessment of human breast and skin tissues. The images captured by the PARS provide contrast and resolution comparable to the gold standard. In PARS images, nuclear organization, connective tissue stroma, and the relationship between highly nuclear cells and connective tissue are highlighted without staining (Fig. 3), whereas H&E staining fails to clearly observe or misses this information. This demonstrates the great potential of PARS as an adjunct to existing histopathological workflows [2]. Moreover, the PARS microscopy can be used as a desktop device for direct histological assessment of unstained embedded tissue.

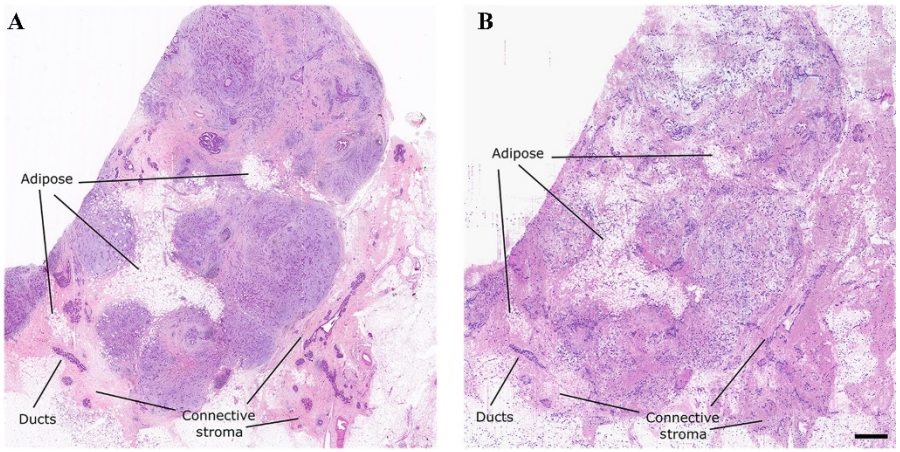

Fig. 3. Comparison of brightfield H&E imaging and the dual-contrast PARS absorption and scattering technique in FFPE human breast tissues in block form. (A) Brightfield image of H&E-stained FFPE tissue sectioned from an FFPE tissue block. (B) Dual-contrast PARS image from the surface of the FFPE human breast tissue block. Scale bar: 1 mm. Adapted with permission from [2] © SPIE.

Biomedical Optics EXPRESS

2.1.3. Coherent Raman scattering microscopy

The low signal intensity of spontaneous Raman scattering has led to advances in nonlinear Raman microscopic methodologies, termed Coherent Raman scattering microscopy. In this process, the Raman scattering intensity is no longer linearly related to the laser intensity. There are two prominent examples, including coherent anti-Stokes Raman scattering (CARS) and stimulated Raman scattering (SRS) microscopy, which can provide fingerprint information of intrinsic vibration on the chemical bonds of molecules, allowing visualization of morphological details and components of cells and tissues on a sub-millimeter scale with high resolution, and high chemical specificity. The Raman signal of SRS arises from the nonlinear interaction between the incident pump and Stokes beams, causing an intensity loss of the pump beam and an intensity gain of the Stokes beam. A significant advantage of SRS is that it is immune to the non-resonant background experienced by CARS. Thus, it is more suitable for imaging living systems. Nowadays, coherent Raman scattering microscopy has brought breakthroughs in biology and medicine, including cellular lipid metabolism, microbiology, protein tumors, and drugs [33,34]. In addition, it has also been successfully applied to rapid and accurate histopathological and intraoperative diagnosis of surgical tissue sections [12,35–39].

In 2013, Ji *et al.* first applied the SRS microscopy to differentiate healthy human and mouse brain tissues from the tumor-infiltrated brain ones based on histoarchitectural and biochemical differences [12]. Experimental results showed that the correlation between SRS microscopy and H&E image for the detection of glioma infiltration was 0.98. In addition, the authors also applied SRS microscopy to visualize tumor margins in mice during surgery, providing rapid intraoperative assessment with improved safety and accuracy of excision. Subsequently, SRS microscopy has been widely used in the histopathology of different tumors and diseases [35–38]. In 2017, Orringer *et al.* developed a portable fiber-laser-based SRS microscope, combing with machine learning of multilayer perceptron, to explore the viability for diagnosis of histopathological images on unprocessed specimens from 101 neurosurgical patients [35]. This technique may be used to render a diagnosis in brain tumor specimens with a high degree of accuracy of 90% and near-perfect concordance with conventional intraoperative histologic techniques. In 2022, Liu *et al.* integrated single-shot femtosecond SRS with U-Net to achieve label-free histology for gastric cancer diagnosis. Fresh endoscopic biopsies were imaged within 60 seconds, showing essential histoarchitectural features in perfect agreement with standard histopathology [36]. In addition to brain tumor diagnosis, SRS has been attempted in gastrointestinal in recent years to precisely reveal the heterogeneous distribution of tumors and their subtypes through semantic segmentation, as shown in Fig. 4 [37,38].

2.1.4. Light sheet microscopy

LSM, also known as selective plane illumination microscopy, originated over a century and has recently seen intense development for rapid biological investigations of relatively transparent specimens [40,41]. It can achieve “optical sectioning” (rejection of out-of-focus light) by using a thin excitation plane of light that irradiates the sample and excites desired signal from an optical plane within the sample, and then the thin plane of the generated signal is probed along a detection axis oriented roughly perpendicular to the light sheet. Compared to conventional microscopy, there is a distinct advantage of the flexible dual-axis configuration of LSM, and illumination and detection paths are coupled and can be individually optimized. In addition to the imaging speed of LSM enables, which is critical for clinical applications, another well-appreciated feature of LSM is that it excites the signal only within the plane of detection, which minimizes photobleaching and photodamage [42–44]. Hence, LSM has been referred to as a desired tool for histopathological diagnosis. However, previous LSM systems were designed to image small non-clinical specimens and were not suitable for imaging large specimens of arbitrary geometry [42–46]. Recently, a number of LSM systems have been developed, including inverted architecture, open-top light

Biomedical Optics EXPRESS

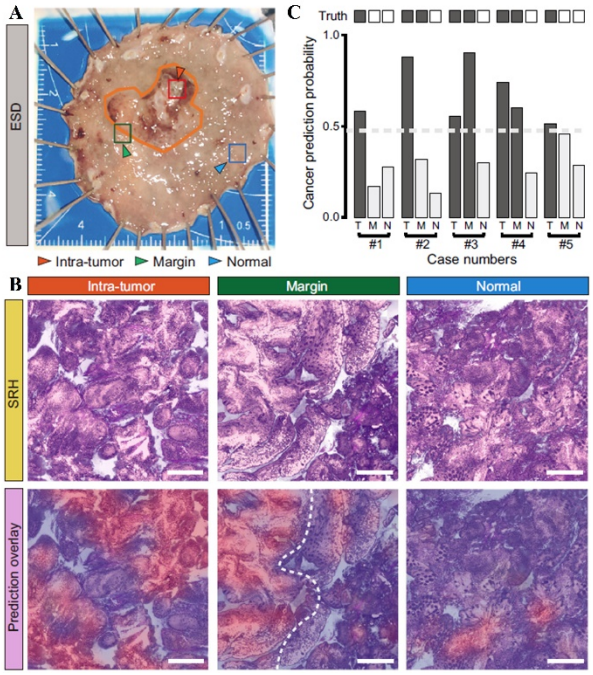

Fig. 4. Intraoperative evaluation of resection margins with convolutional neural network (CNN)-assisted CRSM. (A) A typical endoscopic submucosal dissection (ESD) tissue and three test locations of intra-tumor (T), visual margin (M) and ~8 mm away from the margin (N); (B) SRS imaging results of three test points of a typical case, showing the predicted diagnostic segmentations of cancer (red) vs. non-cancer (blue) (SRH: stimulated Raman histology). (C) SRS prediction results of five ESD cases compared with ground truths. Scale bars: 200 μm. Adapted with permission from Springer Nature: [36].

sheet (OTLS), *etc.*, to accommodate larger specimens with simpler mounting requirements and fewer physical constraints.

Developed by Jonathan Liu's group at the University of Washington, the OTLS microscope was configured like a tissue flatbed scanner and was ideal suited for imaging clinical specimens of various geometries [8,47]. It also provides unconstrained space above the sample, offering the possibility of integrating tissue manipulation accessories such as fluid exchange systems, dissection and aspiration devices to enable high-throughput imaging of pathological images, reducing some of the ambiguities and artifacts encountered when viewing 2D tissue sections of samples. Adam *et al.* explored the utility of OTLS for nondestructive slide-free clinical pathology from fresh human prostate, breast, and kidney tissues, demonstrating a promising histopathological tool of LSM technique to image large human samples within tens of minutes [8]. In addition, a highly versatile design of LSM can provide value as an enhancement to "gold-standard" histopathology for a variety of applications, which confers an advantage of sampling biopsies digitally rather than separating them into tiny fractions. This technique was also demonstrated for rapid evaluation of surgical specimen margin during surgery and can offer cellular resolution without tissue damage [6,48,49]. Figure 5 shows OTLS images of human breast tissues. In 2021, Liu *et al.* further developed a deep learning workflow for prostate cancer risk stratification via nondestructive 3D pathology to assist gland analysis [50].

Biomedical Optics EXPRESS

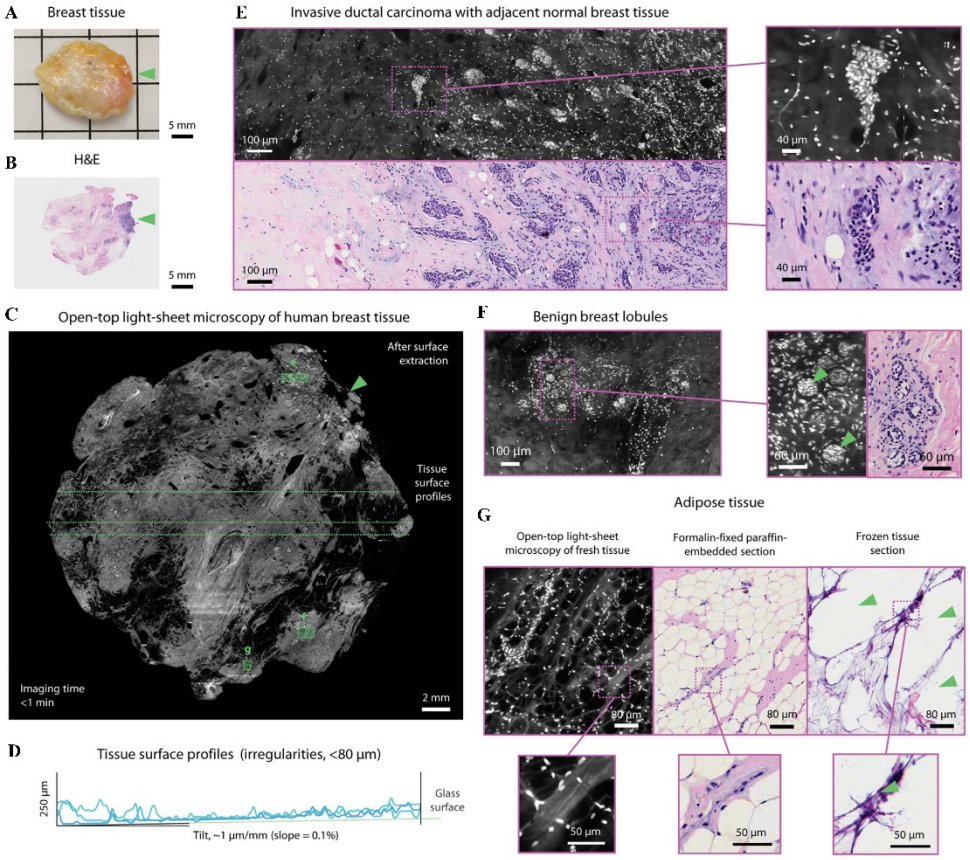

Fig. 5. Rapid intra-operative microscopy of fresh human breast. (A, B) A freshly excised specimen of human breast tissue. (C) Open-top LSM image with representative line profiles of the tissue-surface depth. (D) The inset arrows in (A-C) denote a region of invasive carcinoma. (E) Moderate- and high-magnification images reveal a transition from benign breast tissue to invasive ductal carcinoma. (F) Benign breast lobules are clearly visualized (inset arrows) and correlate with conventional histology. (G) Images of open-top LSM, conventional histology, and frozen-sectioning of fibro-adipose tissue. Adapted with permission from Springer Nature: [8].

2.1.5. Ultraviolet microscopy

Ultraviolet (UV) microscopy, as an important branch of optical microscope, has been rapidly developed and widely used in various applications. It uses UV light to observe samples at a higher resolution than visible light. The light source typically ranges from deep blue to UV wavelengths, with approximately twice the magnification of white light. Currently, there are many types of UV microscopes, such as microscopy with UV surface excitation, reflectance confocal microscopy, *etc*. Using the short wavelength UV light can improve image resolution beyond the diffraction limit of optical microscopes and increase contrast. Motivated by these features, Farzad *et al.* introduced an ultraviolet surface excitation microscopy (MUSE) to obtain high-resolution diagnostic histological images, resembling those obtained from conventional H&E images [51]. This technique can restrict the excitation of conventional fluorescent staining to the tissue surface, without significant effects on downstream molecular detection, including fluorescence *in situ* hybridization and RNA sequencing. In 2023, Zheng *et al.* proposed

Biomedical Optics EXPRESS

dark-field reflectance ultraviolet microscopy (DRUM) to visualize histological images of thick tissues with subcellular resolution and a high signal-to-background ratio in a label-free manner [52]. In DRUM configuration, it enables parallel pixel acquisition, does not require complex mathematical reconstruction, and can provide imaging results for pathological assessment with minimal turnaround time. More importantly, this technique is simple and cost-effective, which may be an ideal tool to enter the surgical room for intraoperative histopathology.

2.2. Computational optical microscopic histopathology

In contrast to dOMH, which has been commercially available for years and has become a routine technique for some applications, cOMH is still performed only in some specialized research labs. As the name suggests, cOMH is a non-WYSIWYG technology. It requires the help of computational imaging technology to obtain the desired image through some algorithmic calculations. The number of cOMH groups has begun to increase in recent years with the development of artificial intelligence techniques and OM. Increasingly, computational optical microscopy is being applied to the field of histopathology, including LFCM, FPM, and PM, *etc*. These techniques, as well as histopathological applications, are summarized in the following sections.

2.2.1. Lens-free computational microscopy

LFCM is based on a front-end acquisition and back-end processing mode, in which a sensor captures the phase change of light passing through the sample in real time and then the sample holographic image is obtained for reconstruction [9,53,54]. By harnessing the coherent plane waves to irradiate the sample, and then capturing the diffraction image of the sample, LFCM allows for imaging thin samples at centimeter scale with high spatial resolution at the submicron level [9,54], making it a powerful technique for high-throughput cellular analysis and bacterial screening, as well as large field-of-view histopathological analysis [54–57]. Combined with a sub-pixel shift-based image super-resolution reconstruction and a multi-height phase recovery algorithm, Greenbaum *et al.* used a LCFM system to achieve large-field-of-view imaging of histopathological slides of invasive breast cancer [57]. The results showed that LFCM can offer sufficient image resolution and contrast for clinic. Compared with pathologist's diagnosis based on conventional microscopy, the overall accuracy can be reached up to 99%. In 2023, Ozcan *et al.* used LFCM technology to acquire holographic images of undyed samples at different times, and then obtained full-field phase images through angular spectrum backpropagation, image stitching, and registration [58]. Figure 6(A) shows lens-free pseudocolor image of human breast carcinoma.

2.2.2. Fourier ptychography microscopy

FPM is a high-throughput computational imaging method that implements the concept of ptychographic scanning in Fourier space [59–61]. In the FPM system, a programmable LED array is adopted to illuminate the sample from different incident angles and the corresponding images are acquired by a low-NA objective lens. During reconstruction, the captured low-resolution intensity images are synthesized in Fourier space to expand the available bandwidth. The synthesized information is then converted back into the spatial domain to generate a high-resolution target image containing intensity and phase attributes, thus avoiding traditional scan stitching artifacts in microscopic-digital pathology of tissue sections and improve imaging throughput and efficiency [59,60]. Yao *et al*. reported a color-transfer FPM for histopathology imaging [61]. Compared with traditional methods, color-transfer FPM sacrifices an average of 0.4% accuracy in exchange for a 2/3 reduction in data acquisition and reconstruction time, which greatly improves the efficiency of color imaging. However, due to the lack of spatial constraints in the color transfer process, this method does not allow for proper staining of samples with two or more dyes. At

Biomedical Optics EXPRESS

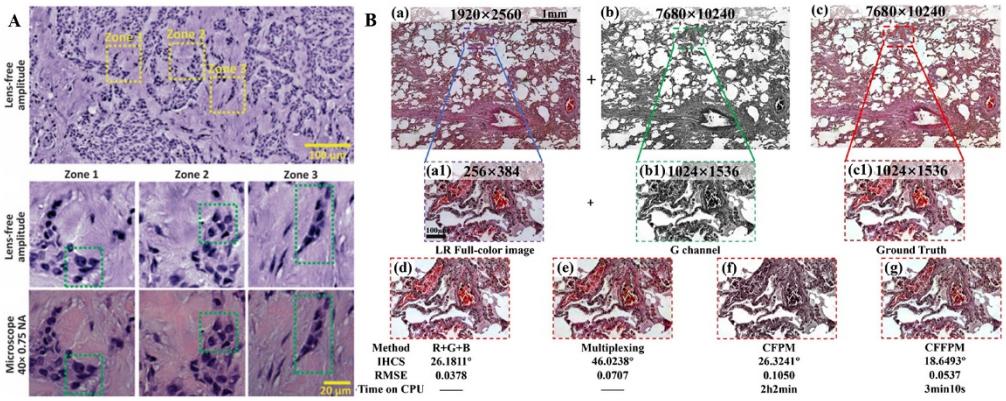

Fig. 6. Histopathological images of LFCM and FPM technologies. (A) Lens-free pseudo-color images of human breast carcinoma. Reprinted with permission from AAAS: [57]. (B) FPM results of stained emphysema, among them, (a) Low-resolution color image; (b) FPM grayscale reconstructed image under green channel; (c) ground truth image. (d-g) Staining images via conventional methods. Adapted with permission from [59] © Optica.

the same time, the histogram matching of individual patches requires a high computational cost. Thus, they further proposed a modified full-color imaging algorithm for FPM in 2022, termed color-transfer filtering FPM [59]. This method combines block processing, trilateral spatial filtering and full-color FPM transfer learning model. The former reduces the search of the solution space, while the latter introduces *a prior* information in the spatial domain, effectively matches the most suitable color-transferred pixels and filters out the noise, and further iterative color refinement through the two-color spaces, thus completely overcoming the important shortcomings of CFPM. The experimental results demonstrated that the method is capable of accurate and rapid color transfer for a wide range of specimens and can provide a turnkey solution for digital pathology (Fig. 6(B)).

2.2.3. Polarization microscopy

PM can identify the anisotropic properties of the fine structure of a substance by utilizing light polarization properties to detect the refractive properties of matter [62,63]. With the help of Mueller matrix, a tool to describe the structure and optical properties of complex tissues, Mueller matrix-based PM (MPM) provides a new solution for disease diagnosis [64–66]. It can offer rich microstructural information of histopathological images, which is suitable for the visualization and analysis of histopathological slides [67,68]. An MPM system is to add a polarization state generator and analyzer (PSG and PSA) on a commercial transmission optical microscope [67], as shown in Fig. 7(A). The forward scattered light emitter by LED passes through the PSG module, the sample module, and the PSA modules in turn, and then the color CCD records conventional hematoxylin and eosin staining images, and the grayscale CCD records a set of polarization intensity images carrying polarization information (Fig. 7(B)). Finally, the Mueller matrix is constructed using the polarization intensity images, and the polarimetric basis parameters are derived for further analysis of the microenvironment of the pathological tissue (Fig. 7(C)).

Currently, MPM provides a window to visualize micro-environmental differences of histopathological samples, thus, it can be used to quantify or grade the cervical intraepithelial neoplasia in human breast cancer at different stages [67,68]. Liu *et al.* explored the correlation between multiple texture features in H&E images and polarization parameters in MPM images of the same sample, providing additional microstructural information for auxiliary diagnosis [67]. Experimental results show that the polarization parameters have the advantage of stably identifying features

Biomedical Optics EXPRESS

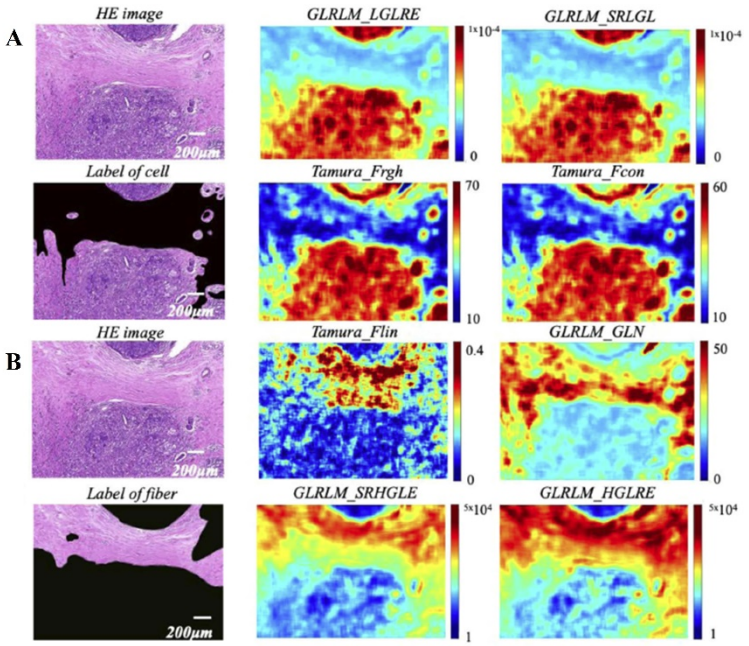

Fig. 7. PM images of breast pathological tissues. Different polarization parameters correspond to cell nuclei (A, labelled with black solid lines in the H&E stained image) and fiber tissue (B, labelled with the red solid lines in the H&E stained image), respectively. Adapted with permission from [67] © The Optica Society.

reflecting tumor progression and inflammation in low-resolution images. Dong *et al.* proposed an MPM-based machine learning for the quantitative diagnosis of cervical precancerous lesions [68]. The experiment achieved cervical intraepithelial neoplasia grading by combing polarized intensity images from MPM with H&E-stained microscopic images to extract regions of interest from the former. It enables interpretable and quantitative diagnosis of cervical precancerous lesions with up to 95% sensitivity and accuracy in a low-resolution and wide-field system. Further, motivated by recent technological advances in PM in conjunction with deep learning, a number of groups have been exploring the value of nondestructive 3D pathology of clinical specimens for diagnosis pathology. Ivan *et al.* developed a multimodal instant polarization microscope (miPolScope) by combining a broadband polarization-resolved detector with reconstruction algorithms [10]. This newly developed miPolScope was demonstrated on myofibril architecture and contractile activity of beating cardiomyocytes, cell and organelle architecture of live HEK293T and U2OS cells. It will facilitate the development of miPolScope in tissue pathology, mechanobiology, and imaging-based-screens.

3. Concluding remarks

OM plays an essential role in revealing tissue types, identifying cancerous tissue from healthy tissue, and necrotic tissue from surviving tissue, *etc*. Its combination with histopathology to form OMH enables fast, cost-effective, high spatial and spectral resolution imaging of tissue sections, opening a new research avenue for histopathology. Histopathological visualization and analysis are one of the current research centers of optical microscopy, where LSFM, PAM, SRS, LSM, UVM, LFCM, FPM, and PM are redefining optics as a potentially routine analytical test. Commercialization of these techniques will enable pathologists to accurately diagnose and excise tumor tissues during surgery. It allows the examination of orders of magnitude more

Biomedical Optics EXPRESS

tissue and enables enhanced quantitative analysis of cell distribution and tissue structure for prognosis and prediction. In addition, advanced optical techniques can simplify laboratory workflow, reduce costs and ensure that samples are available for subsequent molecular testing compared to traditional histological methods. It is foreseeable that OMH is gradually redefining histopathology and optimizing the paradigm of clinical histopathology. Future work could focus on the following aspects.

- with other techniques to provide additional information of histopathology. Individual imaging modalities have limitations in analyzing histopathological data. By combining with advanced OM, new multimodality optical microscopy imaging techniques [69] are expected to make a breakthrough, which can further improve detection diversity, imaging depth and spatial resolution, and thus provide more histopathological information.
- with the advanced artificial intelligent techniques. In order to analyze large feature-rich datasets generated from images, we anticipate that the advances in optical clearing, high-throughput microscopy and artificial intelligent-assisted computational tools will stimulate interest in pathology analysis as a complement to traditional OMH diagnosis. Especially, artificial intelligent technologies will greatly assist the application and promotion of OM in histopathology, including in digital pathology, virtual staining, super-resolution image reconstruction, and intelligent analysis. Deep learning-based prognostic and predictive classification methods are increasingly being applied to this technology.
- to portability and intelligence. The simplicity, portability and intelligence of OMH instruments are critical to the clinical translation of this technology. Especially in application scenarios of clinical real-time intraoperative pathology, miniaturized, portable and intelligent OMH will have more important clinical value and application potential.

Funding. National Key Research and Development Program of China (2022YFB3203800); National Natural Science Foundation of China (62275210, 62105255); National Ten Thousand Talent Program (None); Young Talent Support Program of Shaanxi Province University (None); Key Research and Development Projects of Shaanxi Province (2023-YBSF-293); Fundamental Research Funds for the Central Universities (ZYTS23187).

Disclosures. The authors declare no conflicts of interest.

Data availability. No data were generated or analyzed in the presented research.

References

1. T. Yoshitake, M.G. Giacomelli, L.C. Cahill, D.B. Schmolze, H. Vardeh, B.E. Faulkner, J.L. Connolly, and J.G. Fujimoto, "Direct comparison between confocal and multiphoton microscopy for rapid histopathological evaluation of unfixed human breast tissue," J. Biomed. Opt. **21**(12), 126021 (2016).
2. B. Ecclestone, D. Dinakaran, and P.H. Reza, "Single acquisition label-free histology-like imaging with dual-contrast photoacoustic remote sensing microscopy," J. Biomed. Opt. **26**(05), 056007 (2021).
3. K. Canene-Adams, "Preparation of formalin-fixed paraffin-embedded tissue for immunohidtochemistry," Methods Enzymol. **533**, 225–233 (2013).
4. M. Combalia, S. Garcia, J. Malvehy, S. Puig, A.G. Mulberger, J. Browning, S. Garcet, J.G. Krueger, S.R. Lish, R. Lax, J. Ren, M. Stevenson, N. Doudican, J.A. Carucci, M. Jain, K. White, J. Rakos, and D.S. Gareau, "Deep learning automated pathology in ex vivo microscopy," Biomed. Opt. Express **12**(6), 3103–3116 (2021).
5. Y. Zhang, B.X. Huang, J.J. Wu, and T.W.T. Wong, "Advanced in optical microscopy revolutionize the practice of surgical pathology with rapid and non-destructive tissue assessment," Eur. Phys. J. Spec. Top. **231**(4), 763–779 (2022).
6. J.T.C. Liu, A.K. Glaser, K. Bera, L.D. True, N.P. Reder, K.W. Eliceiri, and A. Madabhushi, "Harnessing non-destructive 3D pathology," Nat. Biomed. Eng. **5**(3), 203–218 (2021).
7. L.C. Cahill, M.G. Giacomelli, T. Yoshitake, H. Vardeh, B.E. Faulkner-Jones, J.L. Conolly, C.K. Sun, and J.G. Fujimoto, "Rapid virtual hematoxylin and eosin histology of breast tissue specimens using a compact fluorescence nonlinear microscope," Lab. Invest. **98**(1), 150–160 (2018).
8. A.K. Glaser, N.P. Reder, Y. Chen, E.F. McCarty, C.B. Yin, L.P. Wei, Y. Wang, L.D. True, and J.T.C. Liu, "Light-sheet microscopy for slide-free non-destructive pathology of large clinical specimens," Nat. Biomed. Eng. **1**(7), 0084 (2017).
9. S.O. Isikman, W. Bishara, S. Mavandadi, F.W. Yu, S. Feng, and R. Lau, "Lens-free optical tomographic microscope with a large imaging volume on a chip," Proc. Natl. Acad. Sci. U. S. A. **108**(18), 7296–7301 (2011).

Biomedical Optics EXPRESS

10. I.E. Ivanov, L.H. Yeh, J.A.P. Bermejo, J.R. Byrum, J.Y.S. Kim, M.D. Leonetti, and S.B. Mehta, "Correlative imaging of the spatio-angular dynamics of biological systems with multimodal instant polarization microscope," Biomed. Opt. Express **13**(5), 3102–3119 (2022).
11. T. T. W. Wong, R.Y. Zhang, P.F. Hai, C. Zhang, M.A. Pleitez, R.L. Aft, D.V. Novack, and L.H.V. Wang, "Fast label-free multilayered histology-like imaging of human breast cancer by photoacoustic microscopy," Sci. Adv. **3**(5), e1602168 (2017).
12. M. Ji, D.A. Orringer, C.W. Freudiger, S. Ramkissoon, X.H. Liu, D. Lau, A.J. Golby, I. Norton, M. Hayashi, N.Y.R. Agar, G.S. Young, C. Spino, S. Santagata, S. Camelo-Piragua, K.L. Ligon, O. Sagher, and X.S. Xie, "Rapid, label-free detection of brain tumors with stimulated Raman scattering microscopy," Sci. Transl. Med. **5**(201), 201ra119 (2013).
13. S. Lin, D. Jheng, K. Hsu, Y. Liu, W. Huang, H. Lee, and C. Tsai, "Rapid pseudo-H&E imaging using a fluorescence-inbuilt optical coherence microscopic imaging system," Biomed. Opt. Express **12**(8), 5139–5158 (2021).
14. D. Kobat, N.G. Horton, and C. Xu, "In vivo two-photon microscopy to 1.6-mm depth in mouse cortex," J. Biomed. Opt. **16**(10), 106014 (2011).
15. J.M. Girkin and G. McConnell, "Advances in laser sources for confocal and multiphoton microscopy," Microsc. Res. Tech. **67**(1), 8–14 (2005).
16. Y. Zhang, L. Kang, I.H.M. Wong, W.X. Dai, X.F. Li, R.C.K. Chan, M.K.Y. Hsin, and T.T.W. Wong, "High-throughput, label-free and slide-free histological imaging by computational microscopy and unsupervised learning," Adv. Sci. **9**(2), 2102358 (2022).
17. E.E. Hoover and J.A. Squier, "Advances in multiphoton microscopy technology," Nat. Photonics **7**(2), 93–101 (2013).
18. N. Akbari, M.R. Rebec, F. Xia, and C. Xu, "Imaging deeper than the transport mean free path with multiphoton microscopy," Biomed. Opt. Express **13**(1), 452–463 (2022).
19. J.V. Chacko and K.W. Eliceiri, "NAD(P)H fluorescence lifetime measurements in fixed biological tissues," Methods Appl. Fluoresc. **7**(4), 044005 (2019).
20. S. Uderhardt, A.J. Martins, J.S. Tsang, T. Lammermann, and R.N. Germain, "Resident macrophages cloak tissue microlesions to prevent neutrophil-driven inflammatory damage," Cell **177**(3), 541–555.e17 (2019).
21. A. Jenett, G.M. Rubin, T.B. Ngo, D. Shepherd, C. Murphy, and H. Dionne, "A GAL4-Driver line resource for drosophila neurobiology," Cell Rep. **2**(4), 991–1001 (2012).
22. G. Leinenga and J. Goetz, "Scanning ultrasound removes amyloid-beta and restores memory in an Alzheimer's disease mouse model," Sci. Transl. Med. **7**(278), 278ra33 (2015).
23. M. Ragazzi, S. Piana, C. Longo, F. Castagnetti, M. Foroni, and G. Ferrari, "Fluorescence confocal microscopy for pathologists," Mod. Pathol. **27**(3), 460–471 (2014).
24. M.M. Zhang, N. Zhong, X. Wang, C.Q. Li, R. Ji, Z. Li, X. Gu, Y.B. Yu, L.X. Li, X.L. Zuo, and Y.Q. Li, "Endoscopic ultrasound-guided needle-based confocal laser endomicroscopy for diagnosis of gastric subepithelial tumors: a pilot study," Endoscopy **51**(06), 560–565 (2019).
25. Z.Y. Qin, C.P. Chen, S.C. He, Y. Wang, K.F. Tam, and N.Y. Lp, "Adaptive optics two-photon endomicroscopy enables deep-brain imaging at synaptic resolution over large volumes," Sci. Adv. **6**(40), eabc6521 (2020).
26. L.M. Schiffhauer, J.N. Boger, T.A. Bonfiglio, J.M. Zavislan, M. Zuley, and C.A. Fox, "Confocal microscopy of unfixed breast needle core biopsies: a comparison to fixed and stained sections," BMC Cancer **9**(1), 265 (2009).
27. D.F. Chen, D.W. Nauen, H.C. Park, D.W. Li, W. Yuan, A. Li, H.H. Guan, C. Kut, K.L. Chaichana, C. Bettegowda, A. Quinones-Hinojosa, and X.D. Li, "Label-free imaging of human brain tissue at subcellular resolution for potential rapid intra-operative assessment of glioma surgery," Theranostics **11**(15), 7222–7234 (2021).
28. L.V. Wang, "Multiscale photoacoustic microscopy and computed tomography," Nat. Photonics **3**(9), 503–509 (2009).
29. S.Y. Liu, X.H. Feng, H.R. Jin, R.C. Zhang, Y.Q. Luo, Z.S. Zheng, and F. Gao, "Handheld photoacoustic imager for theranostics in 3D," IEEE Trans. Med. Imaging **38**(9), 2037–2046 (2019).
30. B. Ecclestone, K. Bell, S. Abbasi, D. Dinakaran, M. Taher, J. Mackey, and P. Haji Reza, "Histopathology for Mohs micrographic surgery with photoacoustic remote sensing microscopy," Biomed. Opt. Express **12**(1), 654–665 (2021).
31. H. Zhang, G. Zhang, Y. Zhang, L. Wen, M. Zhang, J. Pan, P. Wang, X. Wang, Q. Cheng, and X. Wang, "Quantitatively assessing port-wine stains using a photoacoustic imaging method: A pilot study," J. Am. Acad. Dermatol. **85**(6), 1613–1616 (2021).
32. R. Cao, S.D. Nelson, S. Davis, Y. Liang, Y.L. Luo, Y.D. Zhang, B. Crawford, and L.V. Wang, "Label-free intraoperative histology of bone tissue via deep-learning-assisted ultraviolet photoacoustic microscopy," Nat. Biomed. Eng. **7**(2), 124–134 (2022).
33. X.L. Chen, C. zhang, P. Lin, K.C. Huang, J.M. Liang, J. Tian, and J.X. Cheng, "Volumetric chemical imaging by stimulated Raman projection microscopy and tomography," Nat. Commun. **8**(1), 15117 (2017).
34. J. Gagnon, C. Allen, D. Trudel, F. Leblond, P. Stys, C. Brideau, and S. Murugkar, "Spectral focusing-based stimulated Raman scattering microscopy using compact glass blocks for adjustable dispersion," Biomed. Opt. Express **14**(6), 2510–2522 (2023).
35. D.A. Orringer, B. Pandian, Y.S. Niknafs, T.C. Hollon, J. Boyle, and S. Lewis, "Rapid intraoperative histology of unprocessed surgical specimens via fibre-laser-based stimulated Raman scattering microscopy," Nat. Biomed. Eng. **1**(2), 0027 (2017).
36. Z. Liu, W. Su, J. Ao, M. Wang, Q. Jiang, and J. He, "Instant diagnosis of gastroscopic biopsy via deep-learned single-shot femtosecond stimulated Raman histology," Nat. Commun. **13**(1), 4050–4061 (2022).

Biomedical Optics EXPRESS

37. B. Zhang, H. Xu, J. Chen, X. Zhu, Y. Xue, and Y. Yang, "Highly specific and label-free histological identification of microcrystals in fresh human gout tissues with stimulated Raman scattering," Theranostics **11**(7), 3074–3088 (2021).
38. Y. Yang, Y. Yang, Z. Liu, L. Guo, S. Li, and X. Sun, "Microcalcification-based tumor malignancy evaluation in fresh breast biopsies with hyperspectral stimulated Raman scattering," Anal. Chem. **93**(15), 6223–6231 (2021).
39. B.H. Zhang, M.X. Sun, Y.F. Yang, L.C. Chen, X. Zou, T. Yang, Y.Q. Hua, and M.B.A. Ji, "Rapid, large-scale stimulated Raman histology with strip mosaicking and dual-phase detection," Biomed. Opt. Express **9**(6), 2604–2613 (2018).
40. S. Liu, J. Nie, Y.S. Li, T.T. Yu, D. Zhu, and P. Fei, "Three-dimensional, isotropic imaging of mouse brain using multi-view deconvolution light sheet microscopy," J. Innov. Opt. Heal. Sci. **10**(05), 1743006 (2017).
41. M. Rai, C. Li, and A. Greenbaum, "Quantitative analysis of illumination and detection corrections in adaptive light sheet fluorescence microscopy," Biomed. Opt. Express **13**(5), 2960–2974 (2022).
42. J. Huisken and D. Y. R. Stainier, "Even fluorescence excitation by multidirectional selective plane illumination microscopy (mSPIM)," Opt. Lett. **32**(17), 2608–2610 (2007).
43. F.O. Fahrbach, F.F. Voigt, B. Schmid, F. Helmchen, and J. Huisken, "Rapid 3D light-sheet microscopy with a tunable lens," Opt. Express **21**(18), 21010–21026 (2013).
44. S. Yordanov, K. Neuhaus, R. Hartmann, F. Díaz-Pascual, L. Vidakovic, P. Singh, and K. Drescher, "Single-objective high-resolution confocal light sheet fluorescence microscopy for standard biological sample geometries," Biomed. Opt. Express **12**(6), 3372–3391 (2021).
45. D.M. Zhang, G. Yang, Y. Tan, C. Chen, J. Zhang, and H. Li, "Three-dimensional morphological and fluorescent imaging of zebrafish with a continuous-rotational light-sheet microscope," J. Innov. Opt. Heal. Sci. **1**, 2350022 (2023).
46. R.M. Power and J. Huisken, "Intraoperative histology: Lightning 3D histopathology," Nat. Biomed. Eng. **1**(7), 0101 (2017).
47. Y. Chen, W.S. Xie, A.K. Glaser, N.P. Reder, C.Y. Mao, S.M. Dintzis, J.C. Vaughan, and J.T.C. Liu, "Rapid pathology of lumpectomy margins with open open-top light-sheet (OTLS) microscopy," Biomed. Opt. Express **10**(3), 1257–1272 (2019).
48. A.K. Glaser, N.P. Reder, Y. Chen, C.B. Yin, L.P. Wei, S. Kang, L.A. Barner, W.S. Xie, E.F. McCarty, C.Y. Mao, A.R. Halpern, C.R. Stoltzfus, J.S. Daniels, M.Y. Gerner, P.R. Nicovich, J.C. Vaughan, L.D. True, and J.T.C. Liu, "Multi-immersion open-top light-sheet microscope for high-throughput imaging of cleared tissues," Nat. Commun. **10**(1), 2781 (2019).
49. A.K. Glaser, K.W. Bishop, and L.A. Barner, *et al.*, "A hybrid open-top light-sheet microscope for versatile multi-scale imaging of cleared tissues," Nat. Methods **19**(5), 613–619 (2022).
50. W.S. Xie, N.P. Reder, and C. Koyuncu, *et al.*, "Prostate cancer risk stratification via nondestructive 3D pathology with deep learning-assisted gland analysis," Cancer Res. **82**(2), 334–345 (2022).
51. F. Fereidouni, Z.T. Harmany, M. Tian, A. Todd, J.A. Kintner, J.D. McPherson, A.D. Borowsky, J. Bishop, M. Lechpsmmer, and S.G. Demos, "Microscopy with ultraviolet surface excitation for rapid slide-free histology," Nat. Biomed. Eng. **1**(12), 957–966 (2017).
52. S.W. Ye, J.J. Zou, C.M. Huang, F. Xiang, Z.H. Wen, N.M. Wang, J. Yu, Y.Z. He, P. Liu, X. Mei, H. Li, L.L. Niu, P. Gong, and W. Zheng, "Rapid and label-free histological imaging of unprocessed surgical tissues via dark-field reflectance ultraviolet microscopy," iScience **26**(1), 105849 (2023).
53. A. Greenbaum, W. Luo, T.W. Su, Z. Gorocs, L. Xue, and S.O. Isikman, "Imaging without lenes: achievements and remaining challenges of wide-field on-chip microscopy," Nat. Methods **9**(9), 889–895 (2012).
54. Y. Rivenson, Y. Zhang, H. Gunaydm, D. Teng, and A. Ozcan, "Phase recovery and holographic image reconstruction using deep learning in neural networks," Light: Sci. Appl. **7**(2), 17141 (2017).
55. F. Merola, P. Memmolo, L. Miccio, R. Savoia, M. Mugnano, and A. Fontana, "Tomographic flow cytometry by digital holography," Light: Sci. Appl. **6**, e16241 (2016).
56. D. Chen, Z. Wang, K. Chen, Q. Zeng, L. Wang, and X. Xu, "Classification of unlabeled cells using lensless digital holographic images and deep neural networks," Quant. Imag. Med. Surg. **11**(9), 4137–4148 (2021).
57. A. Greenbaum, Y. Zhang, A. Feizi, P. Chung, W. Luo, and S. R. Kandukuri, "Wide-field computational imaging of pathology slides using lens-free on-chip microscopy," Sci. Transl. Med. **6**(267), 267ra175 (2014).
58. T.R. Liu, Y.Z. Li, H.C. Koydemir, Y.J. Zhang, E.T. Yang, M. Eryilmaz, H.D. Wang, J.X. Li, B.J. Bai, G.D. Ma, and A. Ozcan, "Rapid and stain-free quantification of viral plaque via lens-free holography and deep learning," Nat. Biomed. Eng. **7**(8), 1040–1052 (2023).
59. J. R. Chen, A. Y. Wang, A. Pan, G.A. Zheng, C.W Ma, and B.L. Yao, "Rapid full-color Fourier ptychographic microscopy via spatially filtered color transfer," Photonics Res. **10**(10), 2410–2421 (2022).
60. D. Wakefield, R. Graham, K. Wong, S. Wang, C. Hale, and C. Yu, "Cellular analysis using label-free parallel array microscopy with Fourier ptychography," Biomed. Opt. Express **13**(3), 1312–1327 (2022).
61. Y.T. Gao, J.R. Chen, A.Y. Wang, A. Pan, C.W. Ma, and B.L. Yao, "High-throughput fast full-color digital pathology based on Fourier ptychographic microscopy via color transfer," SCI CHINA Phys. Mech. **64**(12), 124251 (2021).
62. V. Lam, T. Phan, K. Ly, X. Luo, G. Nehmetallah, and C. Raub, "Dual-modality digital holographic and polarization microscope to quantify phase and birefringence signals in biospecimens with a complex microstructure," Biomed. Opt. Express **13**(2), 805–823 (2022).

Biomedical Optics EXPRESS

63. K. U. Spandana, K. K. Mahato, and N. Mazumder, "Polarization-resolved Stokes-Mueller imaging: a review of technology and applications," Laser. Med. Sci. **34**(7), 1283–1293 (2019).
64. Y. Wang, H. He, J. Chang, N. Zeng, S. Liu, and M. Li, "Differentiating characteristic microstructural features of cancerous tissues using Mueller matrix microscope," Micron **79**, 8–15 (2015).
65. Y. Dong, J. Qi, H. He, C. He, S. Liu, and J. Wu, "Quantitatively characterizing the microstructural features of breast ductal carcinoma tissues in different progression stages by Mueller matrix microscope," Biomed. Opt. Express **8**(8), 3643–3655 (2017).
66. X. Yang, Q. Zhao, T. Huang, Z. Hu, T. Bu, and H. He, "Deep learning for denoising in a Mueller matrix microscope," Biomed. Opt. Express **13**(6), 3535–3551 (2022).
67. Y. Liu, Y. Dong, L. Si, R. Meng, Y. Dong, and H. Ma, "Comparison between image texture and polarization features in histopathology," Biomed. Opt. Express **12**(3), 1593–1608 (2021).
68. Y. Dong, J. Wan, X. Wang, J. Xue, J. Zou, and H. He, "A polarization-imaging-based machine learning framework for quantitative pathological diagnosis of cervical precancerous lesions," IEEE Trans. Med. Imaging **40**(12), 3728–3738 (2021).
69. Y.P. Li, B.L. Shen, G.J. Zou, R. Hu, Y. Pan, J.L. Qu, and L.W. Liu, "Super-multiplex nonlinear optical imaging unscrambles the statistical complexity of cancer subtypes and tumor microenvironment," Adv. Sci. **9**(5), 2104379 (2022).